SANDIA REPORT
SAND2018-7333
Unlimited Release
Printed June 2018

Correlation of Injury Simulation with Clinical Assessment of Traumatic Brain Injury

Paul A. Taylor, Candice F. Cooper, Andrei A. Vakhtin, Corey C. Ford

Prepared by
Sandia National Laboratories
Albuquerque, New Mexico 87185 and Livermore, California 94550

Sandia National Laboratories is a multimission laboratory managed and operated by National Technology and Engineering Solutions of Sandia, LLC, a wholly owned subsidiary of Honeywell International, Inc., for the U.S. Department of Energy's National Nuclear Security Administration under contract DE-NA0003525.

Issued by Sandia National Laboratories, operated for the United States Department of Energy by National Technology and Engineering Solutions of Sandia, LLC.

Available to DOE and DOE contractors from
U.S. Department of Energy
Office of Scientific and Technical Information
P.O. Box 62
Oak Ridge, TN 37831

Telephone: (865) 576-8401
Facsimile: (865) 576-5728
E-Mail: reports@osti.gov
Online ordering: http://www.osti.gov/scitech

Available to the public from
U.S. Department of Commerce
National Technical Information Service
5301 Shawnee Rd
Alexandria, VA 22312

Telephone: (800) 553-6847
Facsimile: (703) 605-6900
E-Mail: orders@ntis.gov
Online order: https://classic.ntis.gov/help/order-methods/

SAND2018-7333
Printed June 2018
Unlimited Release

Correlation of Injury Simulation with Clinical Assessment of Traumatic Brain Injury

Paul A. Taylor
Candice F. Cooper
Terminal Ballistics Technology
Sandia National Laboratories
P. O. Box 5800
Albuquerque, New Mexico 87185-MS1160

Andrei A. Vakhtin
Corey C. Ford
University of New Mexico Health Sciences Center
MSC10 5620
1 University of New Mexico
Albuquerque, New Mexico 87131-0001

Abstract

This report contains a summary of our efforts to correlate head injury simulations predicting intracranial fluid cavitation with clinical assessments of brain injury from blunt impact to the head. Magnetic resonance imaging (MRI) data, collected on traumatic brain injury (TBI) subjects by researchers at the MIND Institute of New Mexico, was acquired for the current work. Specific blunt impact TBI case histories were selected from the TBI data for further study and possible correlation with simulation. Both group and single-subject case histories were examined. We found one single-subject case that was particularly suited for correlation with simulation. Diffusion tensor image (DTI) analysis of the TBI subject identified white matter regions within the brain displaying reductions in fractional anisotropy (FA), an indicator of local damage to the white matter axonal structures. Analysis of functional magnetic resonance image (fMRI) data collected on this individual identified localized regions of the brain displaying hypoactivity, another indicator of brain injury. We conducted high fidelity simulations of head impact experienced by the TBI subject using the Sandia head-neck-torso model and the shock physics computer code CTH. Intracranial fluid cavitation predictions were compared with maps of DTI fractional anisotropy and fMRI hypoactivity to assess whether a possible correlation exists. The ultimate goal of this work is to assess whether one can correlate simulation predictions of intracranial fluid cavitation with the brain injured sites identified by the fMRI and DTI analyses. The outcome of this effort is described in this report.

ACKNOWLEDGMENTS

This project supported through funding from the Office of Naval Research, Force Health Protection Code 34, C2B2, Dr. Timothy B. Bentley, program manager. The authors wish to thank Dr. Bentley for his support of this project.

TABLE OF CONTENTS

FIGURES

NOMENCLATURE

Abbreviation	Definition
CTH	Shock Physics Computer Simulation Code (not an acronym)
DTI	Diffusion Tensor Imaging
HC	Healthy Controls
FA	Fractional Anisotropy (metric of DTI analysis)
FOV	Field of View (related to magnetic resonance imaging)
fMRI	functional Magnetic Resonance Imaging
ICA	Independent Component Analysis
MNI	Montreal Neurological Institute (defined “standard brain space”)
MRI	Magnetic Resonance Imaging
PCA	Principal Component Analysis (related to fMRI analysis)
ROI	Region of Interest
SNL	Sandia National Laboratories
TBI	Traumatic Brain Injury
TE	Echo time (related to acquisition of MRI data)
TR	Repetition time (related to acquisition of MRI data)
TBSS	Tract-Based Spatial Statistics (aspect of DTI analysis)
UNMHSC	University of New Mexico Health Sciences Center

INTENTIONALLY LEFT BLANK

1. INTRODUCTION

This report contains a summary of our efforts to correlate human injury simulation predictions of impact-induced intracranial fluid cavitation with clinical assessments of brain injury experienced by adult humans as a result of blunt impact to the head. This involved a collaboration between researchers at the University of New Mexico Health Sciences Center (UNMHSC) and Sandia National Laboratories (SNL). The UNMHSC team's first task was to identify human subjects suffering from traumatic brain injury (TBI), as a result of blunt impact, as candidates for injury scenario simulation. In order to perform this task, the UNMHSC team gained access to an existing magnetic resonance imaging (MRI) database, collected by Mayer et al. [1], on TBI subjects. Our intent was to identify those brain injured subjects from the dataset whose injury scenario was fairly well defined and could be recreated via computer simulation. Furthermore, advanced MRI analysis on these subjects, using diffusion tensor imaging (DTI) and functional MRI techniques, had to clearly delineate those regions of the brain displaying structural and/or functional debilitation as a direct result of their blunt force impact injury.

To associate brain injury with predictions of intracranial fluid cavitation, we felt it necessary to study TBI scenarios on a case-by-case basis. If the clinical analysis of single subject case studies displayed measurable brain damage and the injury scenario was amenable to simulation, we would focus on these cases in an effort to correlate our cavitation predictions with observable, clinically measured outcomes. Our modeling and simulation methodology consisted of executing CTH simulations of the injury event experienced by a TBI subject using the Sandia head-neck-torso model. Our goal was to assess whether we could spatially correlate simulation predictions of intracranial fluid cavitation with the brain injured sites identified by the fMRI and DTI analyses collected on the subject. The outcome of this effort is described in this report.

The remainder of this report is partitioned as follows. Section 2 describes our clinical approach in conducting various MRI analyses of TBI data of subjects whose injury scenarios were amenable to computer simulation and possible correlation. Section 3 presents our modeling and simulation methodology and results for a specific TBI injury scenario in which clear clinical evidence of brain injury was evident. Section 4 provides a summary of our correlation work to date and suggested recommendations for further work.

INTENTIONALLY LEFT BLANK

2. CLINICAL ASSESSMENTS OF TRAUMATIC BRAIN INJURY (TBI)

To gather clinical data on traumatic brain injury case histories, our UNMHSC group was granted access to the dataset collected by Mayer et al. [1]. This set consisted of data collected on 48 TBI participants and 48 healthy controls (HC) who were subjected to a series of studies investigating neuronal correlates of semi-acute mild TBI. Quoting from the paper by Mayer et al. [1]: "Inclusion criteria for the TBI group were based on the American Congress of Rehabilitation Medicine, including a Glasgow Coma Score of 13-15 (at first contact with medical staff), loss of consciousness (if present) limited to 30 minutes in duration, and post-traumatic amnesia (if present) limited to 24 hours." In the course of conducting their study, Mayer and colleagues administered a variety of neurocognition tests to the injured cohort in order to arrive at a composite score of emotion and cognition for each subject leading to their diagnosis of TBI. Furthermore, they collected magnetic resonance image data on the TBI subjects using a 3 Tesla Siemens Trio scanner in which both diffusion tensor imaging (DTI) and functional magnetic resonance imaging (fMRI) analyses were collected. Our UNMHSC colleagues (Vakhtin & Ford) conducted additional analyses on the Mayer dataset, the results of which, are described in sections 2.1 and 2.2.

2.1. Mild TBI Group fMRI Analysis

We identified a subgroup of mild TBI patients who sustained non-confounding injuries, excluding those who were involved in a motor vehicle accident or reported multiple head injuries. The aggregate data from the resulting subset of 27 blunt impact, mild TBI subjects along with 27 age/sex-matched healthy controls were decomposed into 100 independent components for functional MRI (fMRI) analysis. We identified previously published networks out of the resulting component set, and subjected them to statistical tests to determine whether network-wise spatial distributions differed between the mild TBI group and the control group. Unfortunately, we did not detect any significant differences between groups following corrections for multiple comparisons. Likewise, we examined the functional network connectivity levels between the two groups, and did not observe any significant group effects. In essence, we found no discernible evidence of brain injury in our mild TBI cohort using functional MRI techniques. Consequently, we focused our attention on the moderate TBI cases which follows next.

2.2. Moderate TBI Analyses

2.2.1. Group Diffusion Tensor Imaging (DTI) Tract-based Spatial Statistics Analysis

We compared white matter integrity across the brain between a group of 6 moderate TBI subjects and age/sex-matched healthy controls. This comparison included the same subjects as the group functional magnetic resonance (fMRI) analysis (which follows) except for one subject who did not undergo diffusion weighted imaging. White matter (WM) tracts common to the entire cohort were first isolated (see Figure 1). Within these WM tracts, we compared fractional anisotropy (FA) values on a voxel-wise basis. We detected no areas displaying significant differences in FA between the TBI cohort and the normal controls following corrections for multiple comparisons. In other words, this

approach did not identify any brain injury with which we could attempt correlation to simulation.

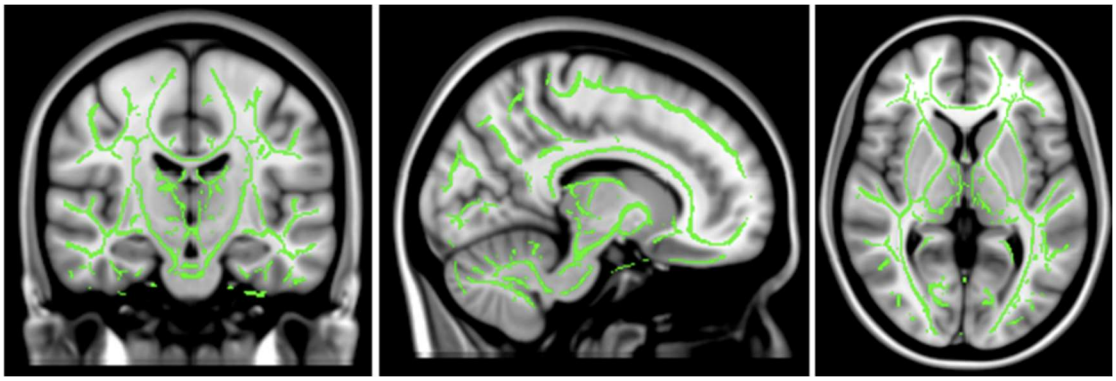

Figure 1. White matter tracts extracted from the entire cohort shown in green. All voxel-wise statistics comparing the TBI patient with healthy controls were conducted within these tracts.

2.2.2. Group functional Magnetic Resonance Imaging (fMRI) Analysis

We analyzed the functional magnetic resonance (fMRI) scans from a group of 7 moderate TBI subjects and 7 healthy control subjects using independent component analysis (ICA) [2], which decomposes aggregate group fMRI data into functional networks that exhibit high levels of intrinsic synchrony, but are maximally statistically independent from other networks. Independent component analysis is a blind source separation algorithm that is used to find statistically independent information based on non-Gaussianity. It does so by estimating the components that linearly mix to form the observed signal. A (*m* x *t)* matrix ***X*** of observed neuroimaging data across *m* locations and *t* time points can therefore be defined as

$$\boldsymbol{X} = \boldsymbol{AS},$$

where ***S*** is an (*n* x *t)* matrix containing *n* components' true source data, and ***A*** is a static (*m* x *n)* mixing-weights matrix that linearly combines source data ***S*** to form the observed signal ***X***. With only ***X*** being known, both ***A*** and ***S*** are undetermined, and need to be estimated by ICA. This is achieved by learning weights in the un-mixing matrix $\boldsymbol{A^{-1}}$, the inverse of ***A***, such that when combined with the observed signal ***X***, features of ***S*** are maximally mutually independent. Accordingly, the equation above can therefore be rearranged as:

$$\boldsymbol{A^{-1}X} = \boldsymbol{S}.$$

The fMRI community has extensively utilized ICA for investigating functional brain networks. Given that fMRI offers more information in the spatial domain of the data, variants of spatial ICA are commonly used for network extraction in this domain. In selecting the appropriate ICA algorithm, the expected source distributions need to be considered, with fMRI sources of interest tending to be non-Gaussian. More specifically, focal fMRI activations have been shown to have super-Gaussian distributions, while artifact-related sources are often sub-Gaussian. This discrepancy presents challenges for

ICA algorithms that are partial to isolating sub- or super-Gaussian sources, as the former would produce a set of nuisance components, while the latter may yield cognition-related components that are contaminated with noise. An algorithm capable of dissociating components with low and high kurtoses is therefore desirable for fMRI decomposition, with the extended Infomax ICA algorithm fitting this criterion. Indeed, both simulation and real fMRI examinations have shown extended Infomax outperforming algorithms like FastICA and JADE in both the estimation of true sources [3] and reliability across multiple runs [4]. Importantly, combinations of preprocessing steps involving principal component analysis (PCA), clustering, and various ICA types have also been contrasted, showing that PCA coupled with spatial extended Infomax yielded the best results [5].

Aggregate group data were decomposed into 50 independent components using the extended Infomax algorithm. Previously published fMRI resting state networks were then selected from the resulting dataset by examining the correlations of spatial distributions between known, previously published networks and every component obtained from the present dataset. Twenty-six such networks were isolated from the 50 extracted components. The spatial distributions of these networks were subsequently compared between the TBI and control groups using a two-sample t-test. Likewise, we contrasted the functional network connectivity levels exhibited by each network pair between the two groups. Functional network connectivity was calculated using a Pearson r-correlation between the time-courses of each network pair. Unfortunately, with this approach, we did not detect any significant statistical differences between TBI and control groups in any of the 26 identified functional networks. Likewise, no group functional connectivity differences were observed in any of the network pairs.

As with the group DTI tract-based analysis reported in the previous section, this approach did not identify any brain injury with which we could attempt correlation to simulation.

2.2.3. Single Subject Diffusion Tensor Imaging (DTI) Tract-based Spatial Statistics Analysis

We identified a single 37-year-old male subject who sustained a moderate blunt trauma to the right parietal lobe and selected this case for a single-subject neuroimaging analysis. According to Mayer [1], the participant was recruited following referral to the Department of Neurosurgery for a post-injury evaluation. We began by examining white matter integrity using the tract-based spatial statistics (TBSS) methodology [6]. Diffusion-weighted scans were obtained with 35 gradient directions. Common white matter tracts were extracted from the study cohort, which included 10 healthy age- and sex-matched control subjects in addition to the participant who sustained the TBI. Within the obtained tracts, voxel-wise values of fractional anisotropy (FA) were compared between the TBI subject and the healthy cohort. The results identified decreases in FA within the cerebellum as well as the white matter underlying the right supplementary motor cortex (see Figure 2).

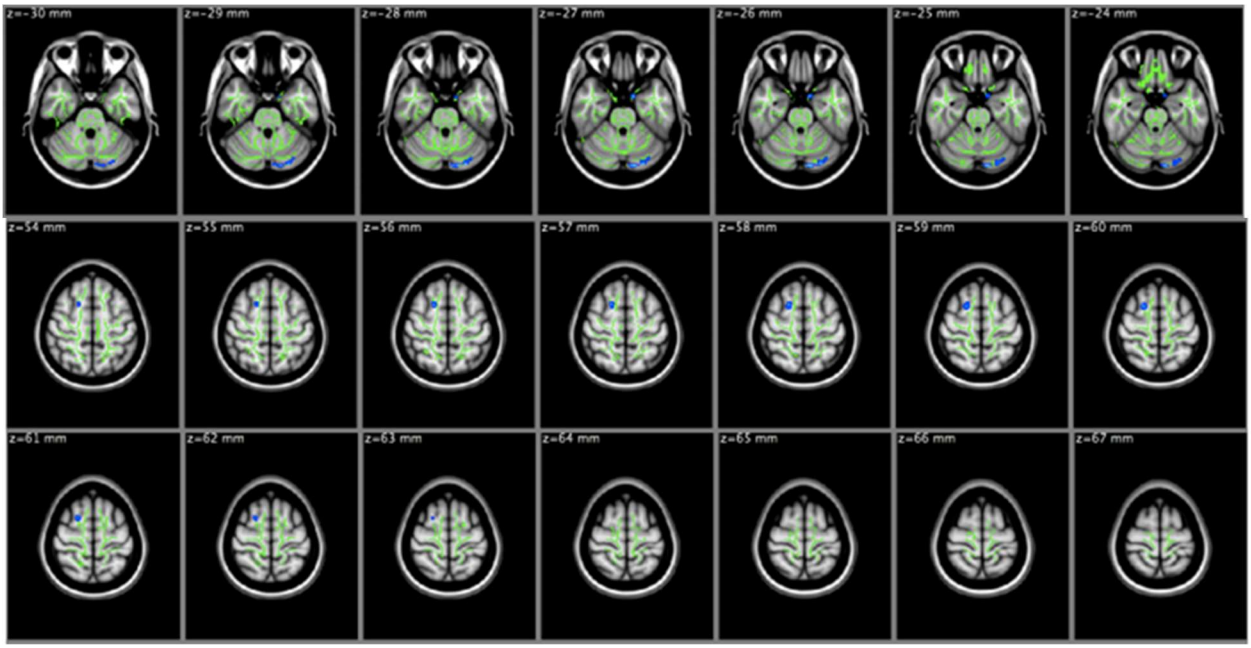

Figure 2. Tract-based spatial statistics (TBSS) results comparing a single parietal impact TBI subject with a group of age and sex-matched healthy controls. Results are filtered using a threshold significance level of p=0.5 and are corrected for multiple comparisons using threshold-free cluster enhancement. Green regions represent the white matter tracts within which all comparisons were conducted. Blue regions specify areas in which the TBI patient displayed decreased levels of fractional anisotropy (FA) relative to controls. The data are presented in radiological space, with the right hemisphere being shown on the left in each image.

2.2.4. Single Subject functional Magnetic Resonance Imaging (fMRI) Analysis

Using independent component analysis (ICA), we decomposed the resting state fMRI data from 11 subjects (1 TBI and 10 healthy controls) into 50 independent components, out of which twenty-three functional networks were identified with the aid of previously described networks [7]. Within each network, two-sample t-tests were conducted to assess any differences in activity levels between the TBI subject and the healthy controls. While no significant differences were detected following a false discovery rate correction for multiple comparisons, results at an uncorrected significance threshold of $p = 0.05$ indicated decreased activity in a sensorimotor network. Specifically, the TBI patient displayed increased activity levels in the left supplementary motor area relative to controls. Additionally, we detected decreased activity levels in the TBI participant's left temporo-frontal network (see Figure 3). The region in the left hemisphere that displayed aberrant elevated activity was homologous to the region that was found to have decreased fractional anisotropy in the right hemisphere.

2.2.5. *Single Subject Diffusion Tensor Image (DTI) Tractography Analysis*

Next, we evaluated white matter integrity within specific tracts that underlie functional networks, derived from fMRI data using ICA, in the single TBI subject suffering blunt injury to the right parietal region. The specification of the tractography seed region used in this approach stands in contrast to previous studies' methodologies, which utilized anatomically defined regions (e. g. based on FreeSurfer cortical parcellations) to isolate known inter-regional tracts. Here, our specification of the seed region is guided by the spatial distribution of the ICA-derived functional network that underlies the suspected area of impact, proximal to the parietal region. Specifically, the region spanned by the right somatomotor functional network was used for sampling streamlines that emanated from it.

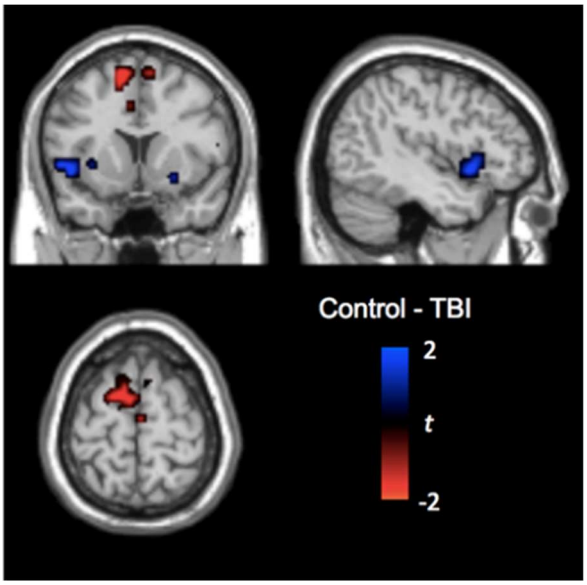

Figure 3. Independent component analysis results comparing a single parietal impact TBI subject with a group of 10 age- and sex-matched healthy controls. The red color specifies the left supplementary motor region on which elevated levels of activity were detected relative to controls. This difference was detected in the sensorimotor network. The blue region near Broca's area displayed decreased activity levels relative to controls and belongs to a larger network that spans the temporo-frontal regions.

Given that the analysis of this particular subject's fMRI data indicated hyperactivity in the somatosensory network contralateral to the injury – possibly reflecting compensatory activity – we hypothesize that aberrant structural connectivity may be present between the left and right somatosensory networks. The right somatomotor network was thus used as the seed region and the left as the tract termination mask.

With the aim of obtaining networks with relatively fine spatial parcellations, we used a high-order fMRI decomposition model, and increased the number of healthy sex-matched control participants to 24. Using the Group ICA of fMRI Toolbox [8], the aggregate fMRI data from our one TBI and 24 control participants were whitened using expectation maximization principle component analysis (PCA) and reduced to 75 principal components. The extended Infomax spatial ICA algorithm was then used to reduce the aggregate data to 75 independent components with maximal statistical independence. Left

and right somatomotor networks were identified in the resulting set of components by examining their spatial distributions and matching them with previously described components. Specifically, Pearson *r* spatial correlation strengths between the *t*-maps of the obtained components and those described in Allen et al. [9] were computed. Those with *R*-values of 0.5 or higher were deemed as candidates for a match, and underwent further visual examinations to confirm positive identifications. As a safeguard against admitting artifact-related components into the final dataset and resolve ambiguities in the case of multiple components representing previously-described ones, low-to-high frequency signal ratios displayed by component activity histograms were also considered. Components with large low-to-high frequency ratios were favored for positive identification, as low ratios are indicative of system noise [7].

Once the somatomotor networks were identified, 99th percentile thresholds of the network's respective *t*-distributions were applied in order to define regions of interest (ROIs) for white matter tractography. The threshold was chosen with the goal of avoiding spatial overlap between ROIs, as well as capturing the centroids that contain most of the voxels that functionally contribute to their respective networks. Further, the ROIs were checked to ensure that they, while residing in the gray matter, did spatially protrude into the white matter for tractography purposes. With the ROIs defined in standard MNI template space [10], we then spatially transformed them to each participant's native space. This was achieved by co-registering the MNI template to the native volumes, and applying the resulting transformation matrices to the two somatosensory ROIs.

Diffusion weighted imaging data were obtained on a Siemens Trio MRI scanner (in one session) producing functional and structural scans. The following parameters were used to obtain the diffusion weighted images: TR = 9 sec, TE = 8.4 sec, voxel size = 2 x 2 x 2 mm^3, 72 slices, FOV = 256 mm, 30 diffusion directions with b = 800 s/mm^2, 5 measurements with b = 0. The diffusion-weighted scans were preprocessed using the FreeSurfer Library (FSL) toolkit [11] for analyzing MRI data. The data was corrected for eddy currents and susceptibility artifacts by removing the difference between diffusion weights obtained via scans in ascending and descending slice order. The diffusion tensor model was then fit to each subject's data. Bayesian estimation of diffusion parameters was performed using sampling techniques while modeling crossing fibers via the BEDPOSTX algorithm [12], which was run on individual subjects' data in native space.

Regions of interest that were previously derived from functional networks were spatially transformed to every subject's native space, and input as seeds and target regions into the probabilistic tracking function PROBTRACKX2 in the FreeSurfer library, which utilized bi-directional tracking algorithms. Each voxel within the seed mask emanated 5000 sample streamlines, and allowed for a maximum voxel-to-voxel streamline curvature of approximately 80 degrees. The built-in "loopcheck" option was used to exclude pathways that looped back onto themselves. The output of the tractography algorithm included the number of pathways that had satisfied the user-specified tracking conditions, and successfully spanned the space between the seed and target masks. The numbers of successful seed-to-target projections obtained from the 24 control participants were used to build a z-distribution, and the single value from the TBI patient was assessed in terms of where it fell on this distribution. The z-test indicated that the TBI patient's structural

connectivity between the left and right somatomotor areas was not significantly different from the control group ($z = -0.926$, $p = 0.354$).

In addition to using the number of successful streamlines sampled from the seed somatosensory region of interest, we examined the mean fractional anisotropies within each participant's isolated tract. In order to address the fact that some subjects exhibit better white matter "trackability" than others, we applied a 90^{th} percentile threshold to the isolated tracts on a subject-wise basis. Those voxels that survived this threshold were used as masks that were applied to each participant's fractional anisotropy (FA) volumes. Mean FA values within these masks were subsequently obtained and contrasted between the TBI patient and the control group. Relative to controls, a z-test indicated a significantly lower mean FA ($z = -2.576$, $p = 0.010$) in the TBI patient within the interhemispheric tract connecting the left and right somatomotor networks.

INTENTIONALLY LEFT BLANK

3. SINGLE TBI SUBJECT INJURY SCENARIO SIMULATION

To associate brain injury with predictions of intracranial fluid cavitation, we felt it necessary to study TBI scenarios on a case-by-case basis. If the clinical analysis of single subject case studies displayed measurable brain damage and the injury scenario was amenable to simulation, then we would investigate these cases in an effort to correlate our cavitation predictions with observable, clinically measured outcomes.

To execute this approach, we simulated the injury scenario experienced by the previously identified single 37-year-old male subject who sustained a moderate blunt trauma to the right parietal lobe. When selecting this TBI subject for study, we felt it important that his case satisfy three requirements. (1) The subject's injury had to be the result of a single event and not the result of multiple insults leading to a cumulative outcome, (2) the clinical assessment of this subject had to identify regions of the brain displaying structural damage and/or functional hypoactivity, and (3) details of the subject's injury scenario had to be understood well enough to be recreated via computer simulation. With these requirements in mind, we selected this particular case for a single-subject neuroimaging assessment including DTI, fMRI, and WM tractography analyses.

To simulate the injury event, we employed the Sandia head-neck-torso model with a subset of the soft tissue torso organs replaced by a single surrogate tissue. This approach was employed to reduce computational overhead while maintaining an adequate amount of bone and soft tissue below the neck to act as a natural boundary condition for the head impact simulations. The head and neck sections retained their original arrangement of organs and bone and remain attached to the torso. The full model consists of 47.2 million cubic elements, each possessing a volume of 1mm x 1mm x 1mm. In the simulation, we introduce a rigid plate whose velocity history was defined to mimic the impact event during the injury scenario (see Figure 4).

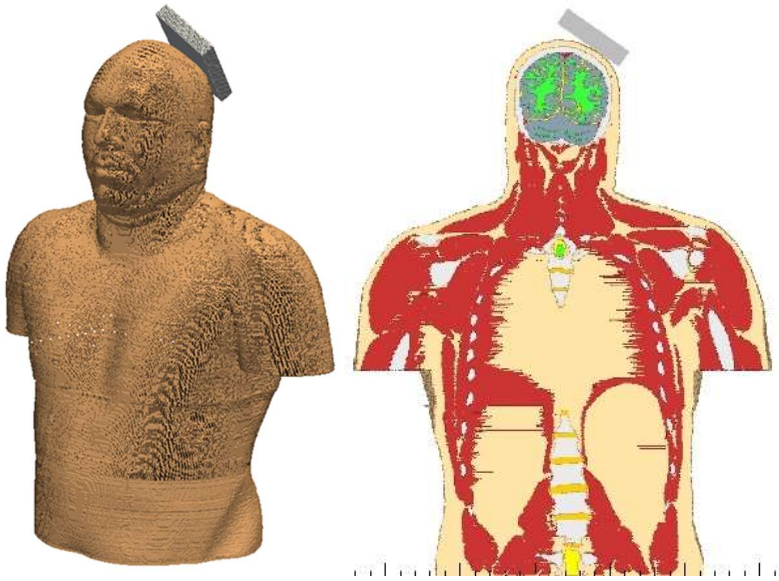

Figure 4. Sandia head-neck-torso model used to simulate head impact mimicking the injury scenario experienced by our single TBI subject. Initial condition of injury scenario: exterior view (left); coronal cut view (right).

In particular, the rigid plate was assigned a velocity history that mimics the fall taken by the TBI subject from a six-foot height onto a hard-packed ground surface. To mimic this event, we specified a rigid plate velocity at 20 ft/sec over a period of zero to 5.15 milliseconds and zero velocity beyond 5.15 milliseconds. The plate impacted the head along a normal to the right rear parietal region, the location identified by our UNMHSC colleagues as the most likely point of impact. Figure 5 illustrates the impact simulation in which pressure is plotted on a coronal section, passing through the midsection of model, as a function of time during the impact event.

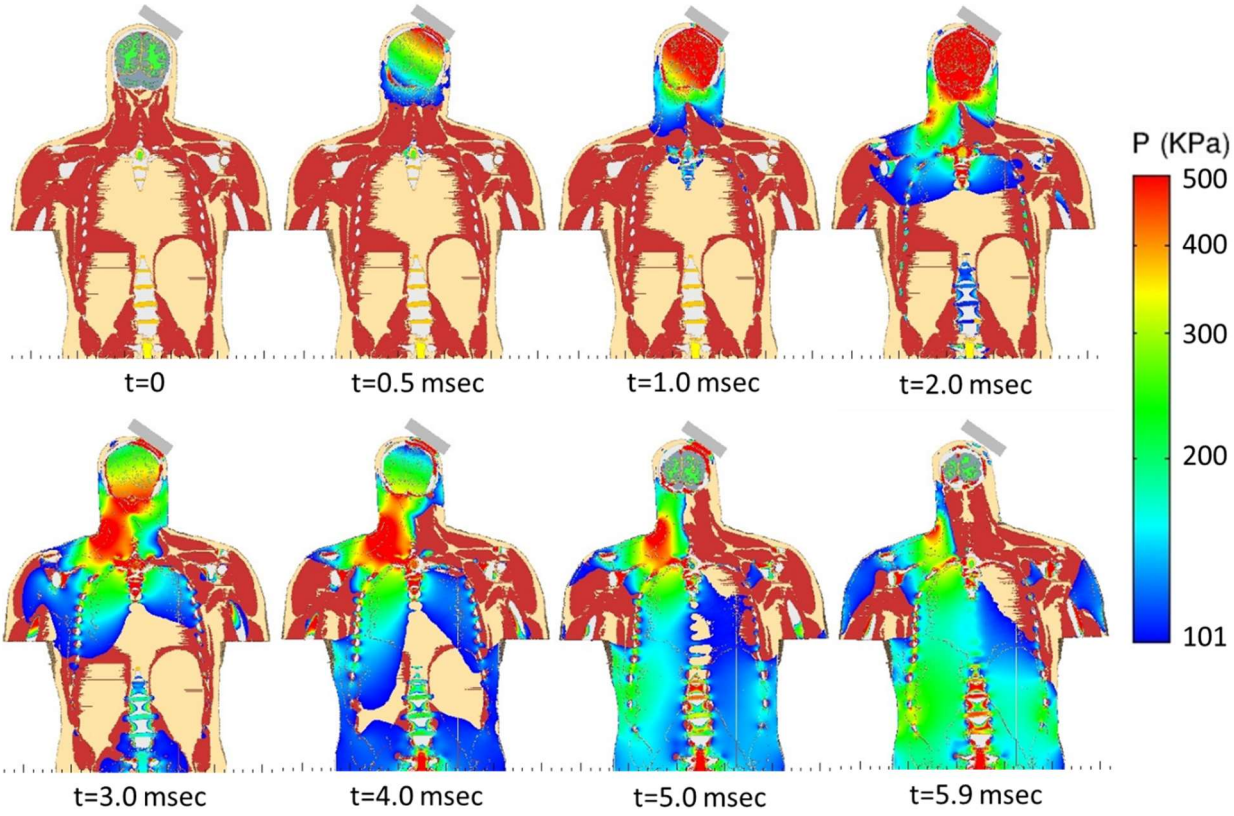

Figure 5. Time lapse images of pressure taken from our simulation of blunt impact leading to TBI in our single subject investigation. These images are generated on a coronal section of the Sandia head-neck-torso model at its midsection. The body rebounds from the impact at a point between the 5.0 and 5.9 milliseconds images.

Recall that our intention is to investigate the connection between intracranial fluid cavitation and localized brain injury. As such, we post-processed our simulations of this event to create spatial maps of fluid cavitation plotted in a series of coronal cut plots for comparison with the clinical DTI and fMRI results. For comparison to the clinical DTI and fMRI brain injury maps, we can create coronal-, sagittal-, and/or axial-cut maps of cavitation vapor volume fraction. These section cuts can be made at spatial intervals of 1 mm, if necessary, through the brain. A small sampling of coronal-cut sections is presented in Figure 6. The plots presented in Figure 6 demonstrate the extent of cavitation predicted to occur within the parietal (Y= 21,22,23,24,25 cm), temporal (Y= 19,20,21 cm), and occipital (Y= 26 cm) regions of the brain and cerebellum proximal to the impact site.

Recall that the diffusion tensor imaging tract-based spatial statistics analysis of this subject identified decreases in FA within the cerebellum as well as the white matter underlying the right supplementary motor cortex (see Figure 2). Our simulation of this event predicted fluid cavitation within both of these regions. Results of our single-subject fMRI independent component analysis identified hypoactivity near Broca's area (blue area in Figure 3) adjacent to the right temporal lobe, a region within which our simulations predict occurrence of cavitation (see Figure 6). Furthermore, the fMRI analysis identified elevated levels of activity (hyperactivity) relative to controls in the left supplementary motor region in an area our simulations did not predict cavitation. This last statement is consistent with the statement that the hyperactive region has not been damaged from the effects of cavitation and can operate at elevated levels of activity to compensate for other areas of the brain that have been damage.

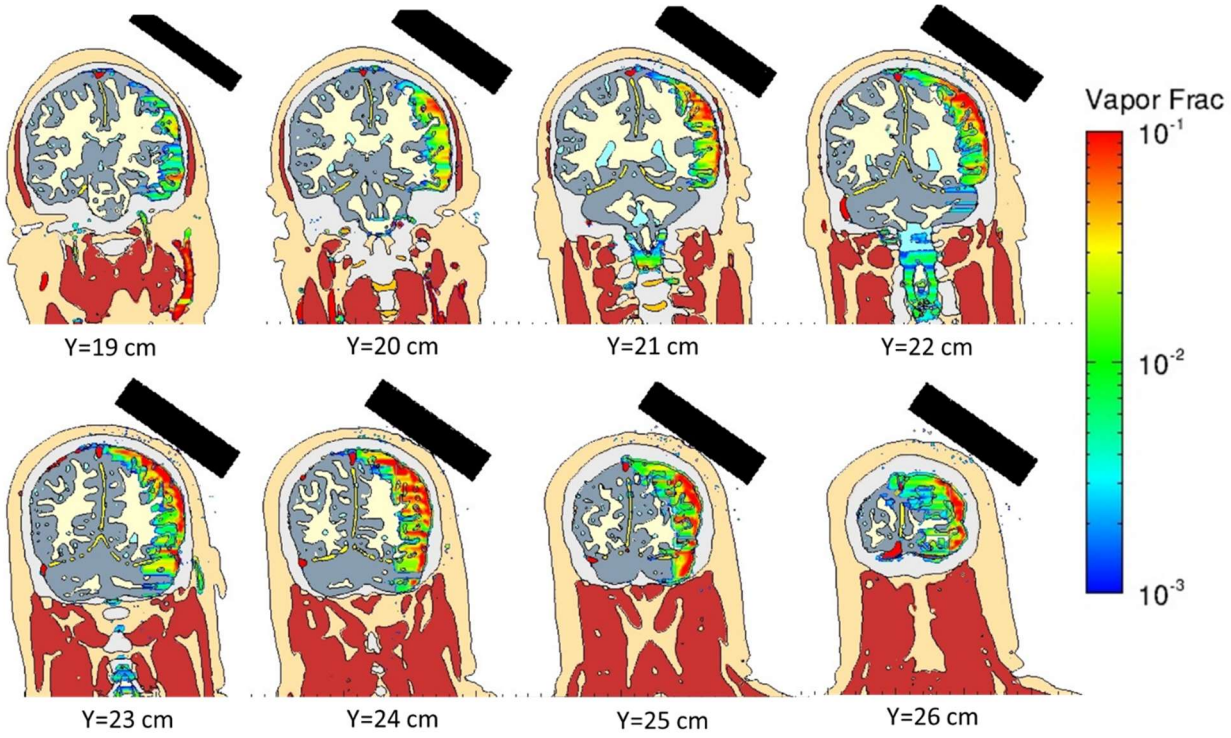

Figure 6. Predictions of maximum cavitation vapor volume fraction plotted in a select number of coronal sections as a result of blunt impact to the left rear parietal region of the head. All plots correspond to the simulation time of 5.9 milliseconds, roughly 0.75 milliseconds after initiation of rebound from the impactor. The coronal cuts are ordered front to back with Y=19 cm to 26 cm.

INTENTIONALLY LEFT BLANK

4. DISCUSSION

To date, we have not attempted to quantify a spatial correlation of our single-subject cavitation predictions with the clinical DTI and fMRI results presented in Figure 2 and Figure 3, identifying regions of the brain displaying structural injury and functional deficits in the parietal and occipital regions of the brain. Although the results from our single subject study are encouraging, far more work needs to be performed on both the clinical and M&S aspects of this project before we can apply statistical methods to attempt correlation of simulation prediction with clinical measurements of TBI. Unfortunately, with the loss of one of our key UNMHSC personnel (Vakhtin), we have had to postpone continuance of this work.

4.1. Suggestions for Further Research

In our opinion, this work should be continued as first proposed. However, there are issues that must be addressed before proceeding. First, and most limiting to such an effort, is gaining access to a large TBI database in order to provide an adequate number of cases to study. The TBI database graciously shared by Mayer and colleagues [1] only provided two candidates for the present study as a result of our stringent screening requirements. This was clearly too small of a sampling of case histories for statistical correlation analysis. Once injury data is available, a more concerted effort must be invested on the clinical side in order to provide an adequate sampling of DTI and fMRI analyses on TBI case histories for correlation to simulation. This last suggestion applies to the modeling and simulation side of the project as well. That is, both the clinical and simulation tasks should be staffed with at least one full time employee on each task (clinical and simulation) to accomplish meaningful results within an acceptable period of time (e.g., 3 years).

Although it is easier to gain access to head impact TBI data, it is also important to investigate the correlation between blast exposure, intracranial fluid cavitation, and TBI. In fact, this topic is of great interest to the military in terms of protecting the warfighter from combat related brain injuries as a result of IED detonation. Unfortunately, it is even more difficult to gain access to blast TBI data for correlation efforts such as the one presented herein.

4.2. Final Comments

The tasks described in this report represent the first steps of an long-term effort to correlate simulation predictions of intracranial fluid cavitation with clinical evidence of brain injury in human subjects suffering from mild TBI. If we or other researchers are eventually successful, the net result would be twofold: (1) impact loading to the head leads to intracranial fluid cavitation and (2) cavitation is a viable brain injury mechanism that warrants further investigation on multiple length scales.

INTENTIONALLY LEFT BLANK

REFERENCES

[1] Mayer, A. R., Ling, J. M., Allen, E. A., Klimaj, S. D., Yeo, R. A., and Hanlon, F. M., 2015, "Static and Dynamic Intrinsic Connectivity Following Mild Traumatic Brain Injury," J. Neurotrauma, **32**, pp. 1046–1055.

[2] Calhoun, V. D., Adali, T., Pearlson, G. D., and Pekar, J. J., 2001, "A Method for Making Group Inferences from Functional MRI Data Using Independent Component Analysis," Hum. Brain Mapp., **14**(3), pp. 140–151.

[3] Correa, N., Adali, T., Li, Y.-O., and Calhoun, V. D., 2005, "Comparison of Blind Source Separation Algorithms for FMRI Using a New Matlab Toolbox: GIFT," *Proceedings. (ICASSP '05). IEEE International Conference on Acoustics, Speech, and Signal Processing, 2005.*, p. v/401-v/404 Vol. 5.

[4] Correa, N., Adali, T., and Calhoun, V. D., 2007, "Performance of Blind Source Separation Algorithms for FMRI Analysis Using a Group ICA Method," Magn. Reson. Imaging, **25**(5), pp. 684–694.

[5] Calhoun, V., Adali, T., and Pearlson, G., 2001, "Independent Component Analysis Applied to fMRI Data: A Generative Model for Validating Results," *Neural Networks for Signal Processing XI, 2001. Proceedings of the 2001 IEEE Signal Processing Society Workshop*, pp. 509–518.

[6] Nakayama, N., Okumura, A., Shinoda, J., Yasokawa, Y.-T., Miwa, K., Yoshimura, S.-I., and Iwama, T., 2006, "Evidence for White Matter Disruption in Traumatic Brain Injury without Macroscopic Lesions," J. Neurol. Neurosurg. Psychiatry, **77**, pp. 850–855.

[7] Allen, E., Erhardt, E. B., Damaraju, E., Gruner, W., Segall, J. M., Silva, R. F., Havlicek, M., Rachakonda, S., Fries, J., Kalyanam, R., Michael, A. M., Caprihan, A., Turner, J. A., Eichele, T., Adelsheim, S., Bryan, A. D., Bustillo, J., Clark, V. P., Feldstein Ewing, S. W., Filbey, F., Ford, C. C., Hutchison, K., Jung, R. E., Kiehl, K. A., Kodituwakku, P., Komesu, Y. M., Mayer, A. R., Pearlson, G. D., Phillips, J. P., Sadek, J. R., Stevens, M., Teuscher, U., Thoma, R. J., and Calhoun, V. D., 2011, "A Baseline for the Multivariate Comparison of Resting-State Networks," Front. Syst. Neurosci., **5**(2), pp. 1–23.

[8] Medical Image Analysis Lab, "GIFT Software," MIALAB [Online]. Available: http://mialab.mrn.org/software/gift/. [Accessed: 01-Aug-2012].

[9] Allen, E. A., Damaraju, E., Plis, S. M., Erhardt, E. B., Eichele, T., and Calhoun, V. D., 2014, "Tracking Whole-Brain Connectivity Dynamics in the Resting State," Cereb. Cortex, **24**(3), pp. 663–676.

[10] Brett, M., Johnsrude, I. S., and Owen, A. M., 2002, "The Problem of Functional Localization in the Human Brain," Nat Rev Neurosci, **3**(3), pp. 243–249.

[11] Dale, A. M., Fischl, B., and Sereno, M. I., 1999, "Cortical Surface-Based Analysis: Segmentation and Surface Reconstruction," NeuroImage, **9**(2), pp. 179–194.

[12] Behrens, T. E. J., Berg, H. J., Jbabdi, S., Rushworth, M. F. S., and Woolrich, M. W., 20007, "Probabillistic Diffusion Tractography with Multiple Fibre Orientation: What Can We Gain?," NeuroImage, **34**, pp. 144–155.

DISTRIBUTION

External:

1 Office of Naval Research, Code 34
Attn: Dr. Timothy Bentley (electronic copy)
875 N. Randolph St.
Arlington, VA 22203P.O. Box 808, MS L-795
timothy.b.bentley@navy.mil

1 The University of New Mexico
Attn: Dr. Corey C. Ford (electronic copy)
MSC10 5620
1 University of New Mexico
Albuquerque, NM 87131-0001
cford@salud.unm.edu

1 Stanford University
Attn: Dr. Andrei A. Vakhtin (electronic copy)
Department of Psychiatry and Behavioral Sciences
Main Administration
401 Quarry Road
Stanford, CA 94305-5717
avakhtin@stanford.edu

Internal:

1	MS1160	Candice F. Cooper	5421 (electronic copy)
1	MS1160	Douglas A. Dederman	5421 (electronic copy)
1	MS1160	Shivonne Haniff	5421 (electronic copy)
1	MS1160	Chad B. Hovey	5421 (electronic copy)
1	MS1160	Ryan J. Terpsma	5421 (electronic copy)
1	MS1160	Kevin P. Ruggirello	5421 (electronic copy)
1	MS1164	Dennis R. Helmich	5420 (electronic copy)
1	MS0899	Technical Library	9536 (electronic copy)

INTENTIONALLY LEFT BLANK


Sandia National Laboratories